

Simple model of active particles

Yann-Edwin Keta

supervised by Joerg Rottler

7/30/18

 [yketa/active_particles](https://github.com/yketa/active_particles)

 [yketa/UBC_2018_Wiki](https://github.com/yketa/UBC_2018_Wiki)



THE UNIVERSITY
OF BRITISH COLUMBIA



1 What is active matter?

2 Model and method

- Model
- Method

3 Observations

- Motility-induced phase separation
- Displacement correlations and cooperativities
- Shear strain correlations

4 Conclusion

Non-equilibrium systems

Three general classes:¹

- Systems relaxing towards equilibrium.

Example

Thermal system adapting to its thermostat, glasses.

¹ Michael E Cates and Julien Tailleur. "Motility-induced phase separation". In: *Annu. Rev. Condens. Matter Phys.* 6.1 (2015), pp. 219–244.

Non-equilibrium systems

Three general classes:¹

- Systems relaxing towards equilibrium.
- Systems with boundary conditions imposing steady currents.

Example

Sheared liquid, metal rod between two thermostats.

¹ Michael E Cates and Julien Tailleur. "Motility-induced phase separation". In: *Annu. Rev. Condens. Matter Phys.* 6.1 (2015), pp. 219–244.

Non-equilibrium systems

Three general classes:¹

- Systems relaxing towards equilibrium.
- Systems with boundary conditions imposing steady currents.
- Active matter.

¹ Michael E Cates and Julien Tailleur. "Motility-induced phase separation". In: *Annu. Rev. Condens. Matter Phys.* 6.1 (2015), pp. 219–244.

Active matter

Definition

System composed of self-driven units, *active particles*, each capable of converting stored or ambient free energy into systematic movement.^a

^aM Cristina Marchetti et al. "Hydrodynamics of soft active matter". In: *Reviews of Modern Physics* 85.3 (2013), p. 1143.

Active matter

Definition

System composed of self-driven units, *active particles*, each capable of converting stored or ambient free energy into systematic movement.^a

^aM Cristina Marchetti et al. "Hydrodynamics of soft active matter". In: *Reviews of Modern Physics* 85.3 (2013), p. 1143.

Example

Cell tissues, swarms of bacteria, schools of fish, flocks of birds.

1 What is active matter?

2 Model and method

- Model
- Method

3 Observations

- Motility-induced phase separation
- Displacement correlations and cooperativities
- Shear strain correlations

4 Conclusion

1 What is active matter?

2 Model and method

- Model
- Method

3 Observations

- Motility-induced phase separation
- Displacement correlations and cooperativities
- Shear strain correlations

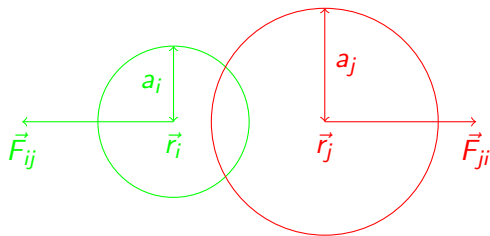
4 Conclusion

Model system

- 2D disks with packing fraction ϕ and 20% polydispersity.

Model system

- 2D disks with packing fraction ϕ and 20% polydispersity.
- Purely repulsive interparticle harmonic potential.

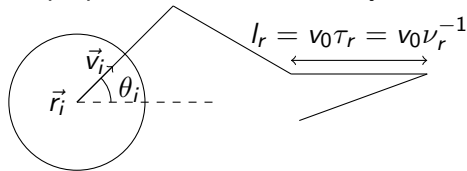


$$\vec{F}_{ij} = \begin{cases} k(a_i + a_j - |\vec{r}_i - \vec{r}_j|)\hat{r}_{ij} & \text{if } a_i + a_j \geq |\vec{r}_i - \vec{r}_j| \\ 0 & \text{otherwise} \end{cases}$$

Yaouen Fily, Silke Henkes, and M Cristina Marchetti. "Freezing and phase separation of self-propelled disks". In: *Soft matter* 10.13 (2014), pp. 2132–2140

Model system

- 2D disks with packing fraction ϕ and 20% polydispersity.
- Purely repulsive interparticle harmonic potential.
- Particle self-propulsion and Brownian dynamics.



$$\frac{d\vec{r}_i}{dt} = \vec{v}_i + \sum_{j \neq i} \vec{F}_{ij} = v_0 \begin{pmatrix} \cos \theta_i \\ \sin \theta_i \end{pmatrix} + \sum_{j \neq i} \vec{F}_{ij}$$

$$\frac{d\theta_i}{dt} = \eta_i(t) ; \langle \eta_i(t) \eta_j(t') \rangle = 2\nu_r \delta_{ij} \delta(t - t')$$

Yaouen Fily, Silke Henkes, and M Cristina Marchetti. "Freezing and phase separation of self-propelled disks". In: *Soft matter* 10.13 (2014), pp. 2132–2140

Model system

- 2D disks with packing fraction ϕ and 20% polydispersity.
- Purely repulsive interparticle harmonic potential.
- Particle self-propulsion and Brownian dynamics.

⇒ 3 control parameters:

Model system

- 2D disks with packing fraction ϕ and 20% polydispersity.
 - Purely repulsive interparticle harmonic potential.
 - Particle self-propulsion and Brownian dynamics.
- ⇒ 3 control parameters:
- packing fraction ϕ ,

Model system

- 2D disks with packing fraction ϕ and 20% polydispersity.
- Purely repulsive interparticle harmonic potential.
- Particle self-propulsion and Brownian dynamics.

⇒ 3 control parameters:

- packing fraction ϕ ,
- dimensionless self-propulsion velocity $\tilde{v} = \frac{v_0}{ak}$,

Model system

- 2D disks with packing fraction ϕ and 20% polydispersity.
- Purely repulsive interparticle harmonic potential.
- Particle self-propulsion and Brownian dynamics.

⇒ 3 control parameters:

- packing fraction ϕ ,
- dimensionless self-propulsion velocity $\tilde{v} = \frac{v_0}{ak}$,
- and dimensionless rotation diffusion constant $\tilde{\nu}_r = \frac{\nu_r}{k}$ or equivalently dimensionless persistence time $\tau_r \equiv \tilde{\nu}_r^{-1}$.

Model system

- 2D disks with packing fraction ϕ and 20% polydispersity.
- Purely repulsive interparticle harmonic potential.
- Particle self-propulsion and Brownian dynamics.

⇒ 3 control parameters:

- packing fraction ϕ ,
 - dimensionless self-propulsion velocity $\tilde{v} = \frac{v_0}{ak}$,
 - and dimensionless rotation diffusion constant $\tilde{\nu}_r = \frac{\nu_r}{k}$ or equivalently dimensionless persistence time $\tau_r \equiv \tilde{\nu}_r^{-1}$.
- Péclet number: $\text{Pe} = \frac{\tilde{v}}{\tilde{\nu}_r} \equiv \text{dimensionless distance travelled before losing orientation.}$

1 What is active matter?

2 Model and method

- Model
- Method

3 Observations

- Motility-induced phase separation
- Displacement correlations and cooperativities
- Shear strain correlations

4 Conclusion

Simulation method

Initialisation

- 20% polydispersity
 - mean radius a , 10 radii in the interval $[0.8a; 1.2a]$
 - uniform radii distribution
- Particles initially randomly positioned
 - then FIRE energy minimisation to decrease interpenetrations

Integration

- Brownian integrator in HOOMD-blue simulation toolkit 

1 What is active matter?

2 Model and method

- Model
- Method

3 Observations

- Motility-induced phase separation
- Displacement correlations and cooperativities
- Shear strain correlations

4 Conclusion

1 What is active matter?

2 Model and method

- Model
- Method

3 Observations

- Motility-induced phase separation
- Displacement correlations and cooperativities
- Shear strain correlations

4 Conclusion

Spontaneous phase separation

$N = 2.00e + 03, \phi = 0.50, \tilde{V} = 1.00e - 02, \tilde{V}_r = 5.00e - 06, L = 1.128e + 02$
 $t = 0.00000e + 00, \Delta t = 5.00000e + 02$

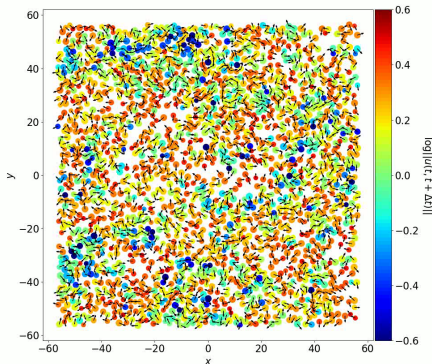


Figure: (Movie) Spontaneous phase separation in our active system. $\vec{u}(t, t + \Delta t)$ \equiv particle displacement between times t and $t + \Delta t$.

Motility-induced phase separation

Definition

Phase separated state arising in systems of motile particles which speed decreases sufficiently steeply with increasing local density.
A dilute active gas coexists with a dense liquid of substantially reduced motility.

Michael E Cates and Julien Tailleur. "Motility-induced phase separation". In: *Annu. Rev. Condens. Matter Phys.* 6.1 (2015), pp. 219–244

Motility-induced phase separation

Figure: Motility-induced phase separation mechanism diagram.

Michael E Cates and Julien Tailleur. "Motility-induced phase separation". In: *Annu. Rev. Condens. Matter Phys.* 6.1 (2015), pp. 219–244

Motility-induced phase separation

particles accumulating where they move more slowly

Figure: Motility-induced phase separation mechanism diagram.

Michael E Cates and Julien Tailleur. "Motility-induced phase separation". In: *Annu. Rev. Condens. Matter Phys.* 6.1 (2015), pp. 219–244

Motility-induced phase separation

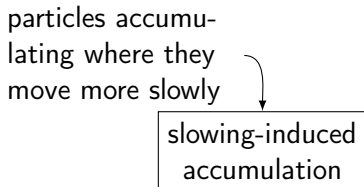


Figure: Motility-induced phase separation mechanism diagram.

Michael E Cates and Julien Tailleur. "Motility-induced phase separation". In: *Annu. Rev. Condens. Matter Phys.* 6.1 (2015), pp. 219–244

Motility-induced phase separation

particles accumu-
lating where they
move more slowly



slowing-induced
accumulation

density-dependent
self-propulsion
velocity

Figure: Motility-induced phase separation mechanism diagram.

Michael E Cates and Julien Tailleur. "Motility-induced phase separation". In: *Annu. Rev. Condens. Matter Phys.* 6.1 (2015), pp. 219–244

Motility-induced phase separation

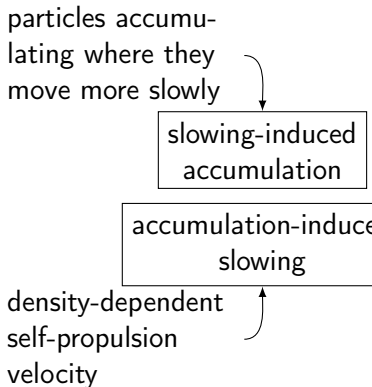


Figure: Motility-induced phase separation mechanism diagram.

Michael E Cates and Julien Tailleur. "Motility-induced phase separation". In: *Annu. Rev. Condens. Matter Phys.* 6.1 (2015), pp. 219–244

Motility-induced phase separation

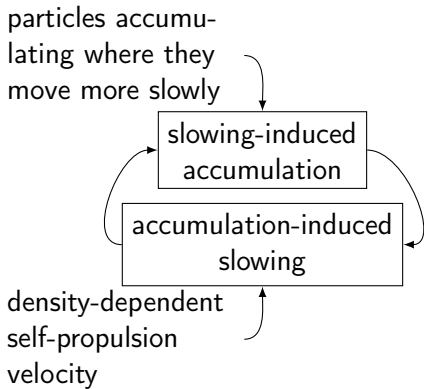


Figure: Motility-induced phase separation mechanism diagram.

Michael E Cates and Julien Tailleur. "Motility-induced phase separation". In: *Annu. Rev. Condens. Matter Phys.* 6.1 (2015), pp. 219–244

Motility-induced phase separation

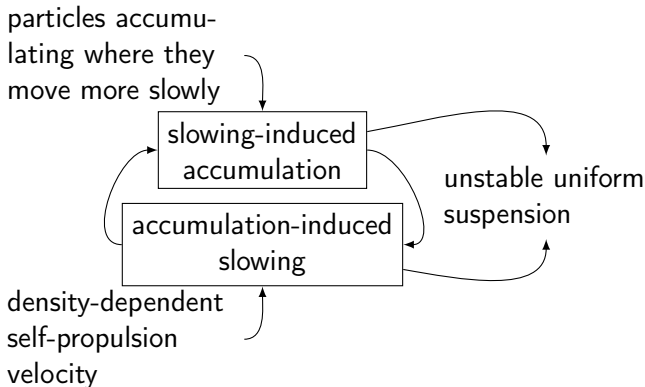


Figure: Motility-induced phase separation mechanism diagram.

Michael E Cates and Julien Tailleur. "Motility-induced phase separation". In: *Annu. Rev. Condens. Matter Phys.* 6.1 (2015), pp. 219–244

Motility-induced phase separation

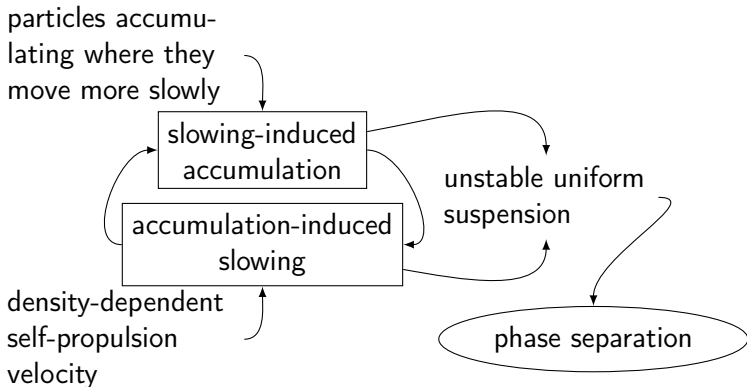


Figure: Motility-induced phase separation mechanism diagram.

Michael E Cates and Julien Tailleur. "Motility-induced phase separation". In: *Annu. Rev. Condens. Matter Phys.* 6.1 (2015), pp. 219–244

Phase diagram at fixed $\tilde{\nu}_r$

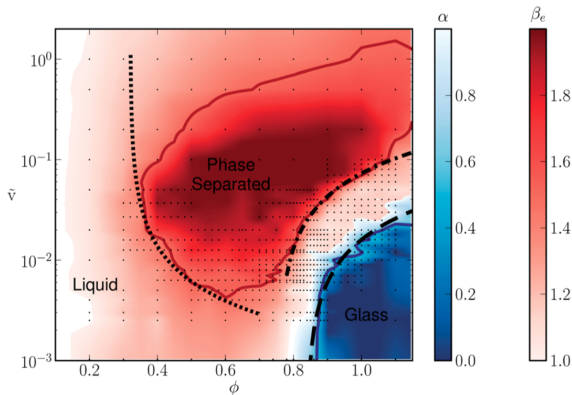


Figure: Phase diagram for $\tilde{\nu}_r = 5 \cdot 10^{-4}$.²

²Yaouen Fily, Silke Henkes, and M Cristina Marchetti. "Freezing and phase separation of self-propelled disks". In: *Soft matter* 10.13 (2014), pp. 2132–2140.

Phase diagram at fixed $\tilde{\nu}_r$

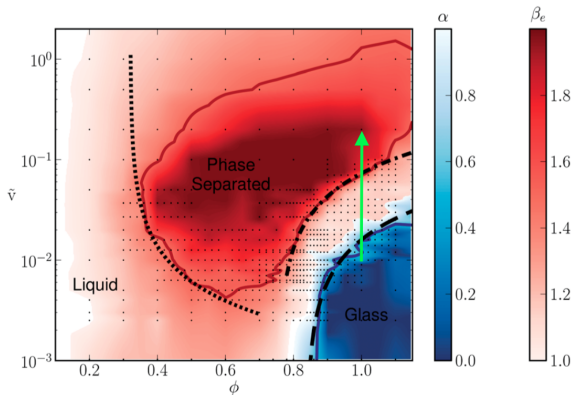


Figure: Phase diagram for $\tilde{\nu}_r = 5 \cdot 10^{-4}$.²

²Yaouen Fily, Silke Henkes, and M Cristina Marchetti. "Freezing and phase separation of self-propelled disks". In: *Soft matter* 10.13 (2014), pp. 2132–2140.

Local density distribution with varying \tilde{v}

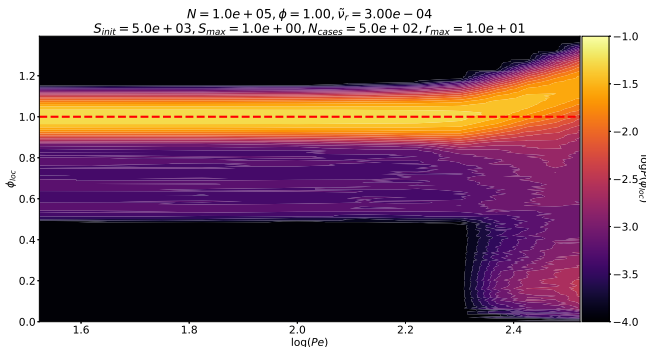


Figure: Histogram of local density ϕ_{loc} with varying self-propulsion velocity \tilde{v} , at packing fraction $\phi = 1.00$ and rotation diffusion constant $\tilde{\nu}_r = 3 \cdot 10^{-4}$.

Phase diagram boundaries with varying $\tilde{\nu}_r$

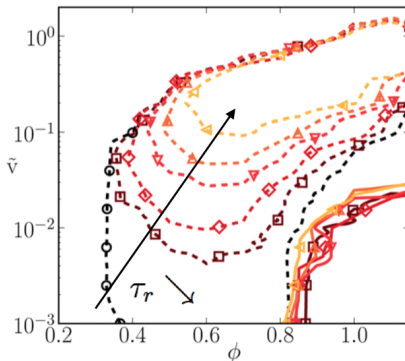


Figure: Boundaries of glassy (solid lines) and phase separated (dashed lines) regions for different persistence times τ_r .³

³ Yaouen Fily, Silke Henkes, and M Cristina Marchetti. "Freezing and phase separation of self-propelled disks". In: *Soft matter* 10.13 (2014), pp. 2132–2140.

Phase diagram boundaries with varying $\tilde{\nu}_r$

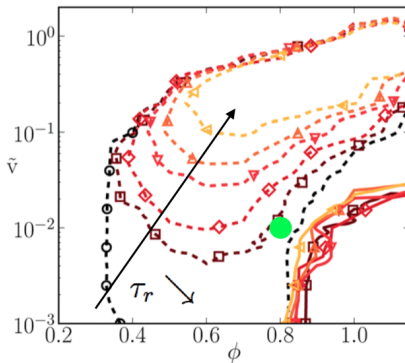


Figure: Boundaries of glassy (solid lines) and phase separated (dashed lines) regions for different persistence times τ_r .³

³ Yaouen Fily, Silke Henkes, and M Cristina Marchetti. "Freezing and phase separation of self-propelled disks". In: *Soft matter* 10.13 (2014), pp. 2132–2140.

Local density distribution with varying $\tilde{\nu}_r$

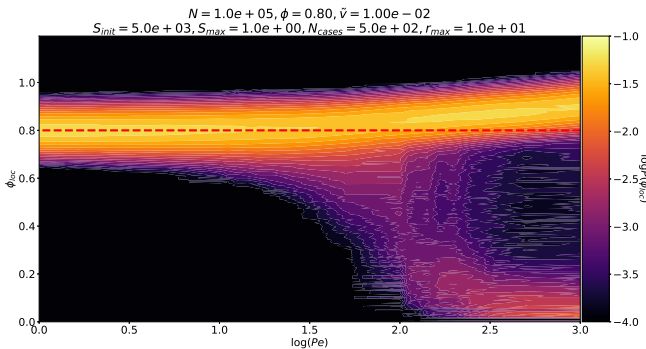


Figure: Histogram of local density ϕ_{loc} with varying rotation diffusion constant $\tilde{\nu}_r$, at packing fraction $\phi = 0.80$ and rotation diffusion constant $\tilde{\nu} = 1 \cdot 10^{-2}$.

1 What is active matter?

2 Model and method

- Model
- Method

3 Observations

- Motility-induced phase separation
- **Displacement correlations and cooperativities**
- Shear strain correlations

4 Conclusion

Displacement map at low activity

$N = 1.00e + 05, \phi = 0.80, \tilde{\nu} = 1.00e - 02, \tilde{\nu}_r = 1.00e - 02, L = 6.308e + 02, L_{new} = 1.000e + 02$
 $t = 5.0000e + 04, \Delta t = 1.0000e + 02$

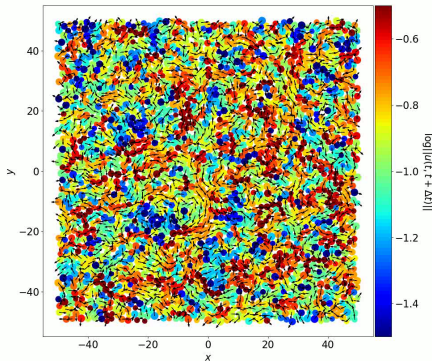


Figure: (Movie) Displacement maps at low activity ($\tilde{\nu}_r = 1 \cdot 10^{-2}$) with $\tilde{\nu}_r \Delta t = 1$.
 $\vec{u}(t, t + \Delta t) \equiv$ particle displacement between times t and $t + \Delta t$.

Displacement map at high activity

$$N = 1.00e + 05, \phi = 0.80, \tilde{\nu} = 1.00e - 02, \tilde{\nu}_r = 2.00e - 05, L = 6.308e + 02, L_{new} = 1.000e + 02 \\ t = 5.00000e + 06, \Delta t = 5.00000e + 04$$

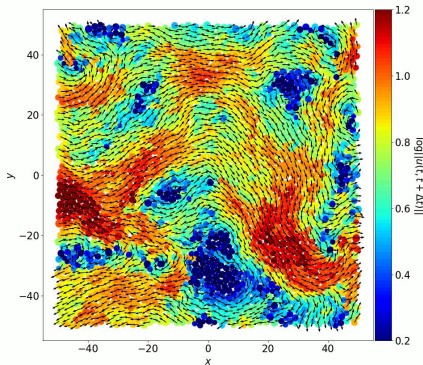


Figure: (Movie) Displacement maps at high activity ($\tilde{\nu}_r = 2 \cdot 10^{-5}$) with $\tilde{\nu}_r \Delta t = 1$.
 $\vec{u}(t, t + \Delta t) \equiv$ particle displacement between times t and $t + \Delta t$.

Displacement correlation

$\vec{u}(\vec{r}, t, t + \Delta t) \equiv$ displacement of particle at position \vec{r} between times t and $t + \Delta t$

$$C_{uu}(\Delta \vec{r}, \Delta t) = \langle \vec{u}(\vec{r} + \Delta \vec{r}, t, t + \Delta t) \cdot \vec{u}(\vec{r}, t, t + \Delta t) \rangle$$

Displacement correlation

$\vec{u}(\vec{r}, t, t + \Delta t) \equiv$ displacement of particle at position \vec{r} between times t and $t + \Delta t$

$$\begin{aligned} C_{uu}(\Delta \vec{r}, \Delta t) &= \langle \vec{u}(\vec{r} + \Delta \vec{r}, t, t + \Delta t) \cdot \vec{u}(\vec{r}, t, t + \Delta t) \rangle \\ &= \frac{\int dt \int d^2 \vec{r} \vec{u}(\vec{r}, t, t + \Delta t) \cdot \vec{u}(\vec{r} + \Delta \vec{r}, t, t + \Delta t)}{\int dt \int d^2 \vec{r} ||\vec{u}(\vec{r}, t, t + \Delta t)||^2} \end{aligned}$$

Displacement correlation

$\vec{u}(\vec{r}, t, t + \Delta t) \equiv$ displacement of particle at position \vec{r} between times t and $t + \Delta t$

$$\begin{aligned} C_{uu}(\Delta\vec{r}, \Delta t) &= \langle \vec{u}(\vec{r} + \Delta\vec{r}, t, t + \Delta t) \cdot \vec{u}(\vec{r}, t, t + \Delta t) \rangle \\ &= \frac{\int dt \int d^2\vec{r} \vec{u}(\vec{r}, t, t + \Delta t) \cdot \vec{u}(\vec{r} + \Delta\vec{r}, t, t + \Delta t)}{\int dt \int d^2\vec{r} ||\vec{u}(\vec{r}, t, t + \Delta t)||^2} \\ &= \frac{\mathcal{F}^{-1}\left\{\int dt ||\mathcal{F}\{\vec{u}\}(\vec{k}, t, t + \Delta t)||^2\right\}(\Delta\vec{r}, \Delta t)}{\int dt \int d^2\vec{r} ||\vec{u}(\vec{r}, t, t + \Delta t)||^2} \end{aligned}$$

Displacement correlation

$\vec{u}(\vec{r}, t, t + \Delta t) \equiv$ displacement of particle at position \vec{r} between times t and $t + \Delta t$

$$\begin{aligned} C_{uu}(\Delta\vec{r}, \Delta t) &= \langle \vec{u}(\vec{r} + \Delta\vec{r}, t, t + \Delta t) \cdot \vec{u}(\vec{r}, t, t + \Delta t) \rangle \\ &= \frac{\int dt \int d^2\vec{r} \vec{u}(\vec{r}, t, t + \Delta t) \cdot \vec{u}(\vec{r} + \Delta\vec{r}, t, t + \Delta t)}{\int dt \int d^2\vec{r} \|\vec{u}(\vec{r}, t, t + \Delta t)\|^2} \\ &= \frac{\mathcal{F}^{-1}\{\int dt \|\mathcal{F}\{\vec{u}\}(\vec{k}, t, t + \Delta t)\|^2\}(\Delta\vec{r}, \Delta t)}{\int dt \int d^2\vec{r} \|\vec{u}(\vec{r}, t, t + \Delta t)\|^2} \end{aligned}$$

$$C_{uu}(\Delta\vec{r}, \Delta t) \xrightarrow{\text{isotropy}} C_{uu}(\Delta r, \Delta t)$$

Necessity of dividing by density correlation

Displacements are put on a grid to calculate their correlations.

$$\vec{u}(\vec{r}_i, t, t + \Delta t) \xrightarrow{\text{coarse-graining}} \vec{u}_{ij}(t, t + \Delta t)$$

(average in grid box)

Necessity of dividing by density correlation

Displacements are put on a grid to calculate their correlations.

$$\vec{u}(\vec{r}_i, t, t + \Delta t) \xrightarrow[\text{coarse-graining}]{\text{(average in grid box)}} \vec{u}_{ij}(t, t + \Delta t) \xrightarrow{\text{FFT}} C_{uu,ij}$$

Necessity of dividing by density correlation

Displacements are put on a grid to calculate their correlations.

$$\vec{u}(\vec{r}_i, t, t + \Delta t) \xrightarrow[\text{(average in grid box)}]{\text{coarse-graining}} \vec{u}_{ij}(t, t + \Delta t) \xrightarrow{\text{FFT}} C_{uu,ij}$$

Issue: small grid spacing \Rightarrow significant amount of grid boxes are empty.

Necessity of dividing by density correlation

Displacements are put on a grid to calculate their correlations.

$$\vec{u}(\vec{r}_i, t, t + \Delta t) \xrightarrow[\text{(average in grid box)}]{\text{coarse-graining}} \vec{u}_{ij}(t, t + \Delta t) \xrightarrow{\text{FFT}} C_{uu,ij}$$

Issue: small grid spacing \Rightarrow significant amount of grid boxes are empty.

$$\rho_{ij} = \begin{cases} 1 & \text{if } \vec{u}_{ij} \neq \vec{0} \\ 0 & \text{otherwise} \end{cases} \equiv \text{density}$$

Small grid spacing \Rightarrow significant amount of ρ_{ij} are equal to 0.

Necessity of dividing by density correlation

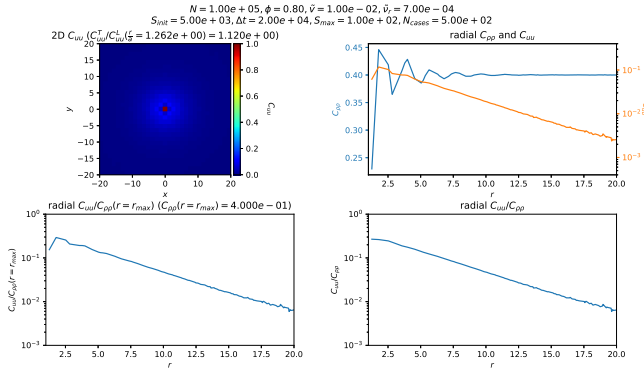


Figure: Displacement correlations $C_{uu}(r, \Delta t)$ and density correlations $C_{\rho\rho}(r)$, at packing fraction $\phi = 0.80$, self-propulsion velocity $\tilde{v} = 1 \cdot 10^{-2}$, and rotation diffusion constant $\tilde{\nu}_r = 7 \cdot 10^{-4}$.

→ $C_{uu,ij}$ has to be divided by $C_{\rho\rho,ij} \propto$ radial distribution function.

Displacement correlation

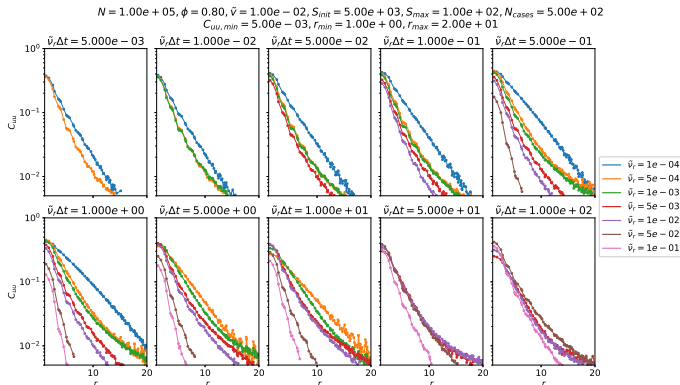


Figure: Comparison of displacement correlations $C_{uu}(r, \Delta t)$ for equal numbers of rotations $\tilde{v}_r\Delta t$, at packing fraction $\phi = 0.80$ and self-propulsion velocity $\tilde{v} = 1 \cdot 10^{-2}$.

Displacement cooperativity

$$\chi(\Delta t, r_{min}, r_{max}) = \frac{1}{L^2} \int_{r=r_{min}}^{r=r_{max}} dr 2\pi r C_{uu}(r, \Delta t)$$

with L the characteristic length of the system.

Definition

$\chi \equiv$ average proportion of particles acting as coherently moving neighbours → measure of dynamical heterogeneity.

Adam Wysocki, Roland G Winkler, and Gerhard Gompper. "Cooperative motion of active Brownian spheres in three-dimensional dense suspensions". In: *EPL (Europhysics Letters)* 105.4 (2014), p. 48004

Burkhard Doliwa and Andreas Heuer. "Cooperativity and spatial correlations near the glass transition: Computer simulation results for hard spheres and disks". In: *Physical Review E* 61.6 (2000), p. 6898



Displacement cooperativity with varying $\tilde{\nu}_r$

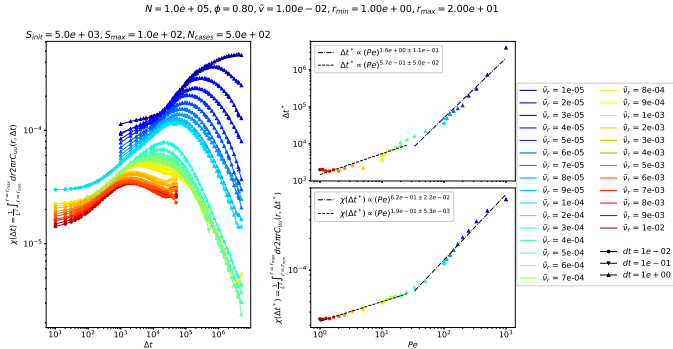


Figure: Comparison of displacement cooperativities $\chi(\Delta t)$, times of maximum cooperativity Δt^* and maximum cooperativities $\chi(\Delta t^*)$, at packing fraction $\phi = 0.80$ and self-propulsion velocity $\tilde{\nu} = 1 \cdot 10^{-2}$.

- Clear change of $\Delta t^*(Pe)$ and $\chi(\Delta t^*, Pe)$ slopes at MIPS.
- $(\tau_r \nearrow \Leftrightarrow Pe \nearrow) \Rightarrow \Delta t^* \nearrow, \chi(\Delta t^*) \nearrow$

Displacement cooperativity with varying $\tilde{\nu}_r$

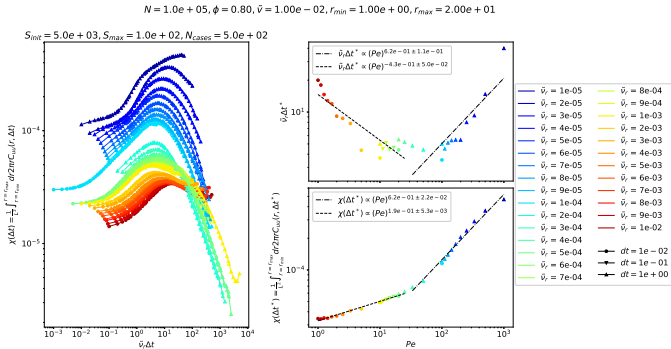


Figure: Comparison of displacement cooperativities $\chi(\Delta t)$, number of rotations of maximum cooperativity $\tilde{\nu}_r \Delta t^*$ and maximum cooperativities $\chi(\Delta t^*)$, at packing fraction $\phi = 0.80$ and self-propulsion velocity $\tilde{\nu} = 1 \cdot 10^{-2}$.

- Clear change of $\tilde{\nu}_r \Delta t^*(\text{Pe})$ and $\chi(\Delta t^*, \text{Pe})$ slopes at MIPS.
- Non-monotonous variations of $\tilde{\nu}_r \Delta t^*$ with Pe .

Ageing effect with varying $\tilde{\nu}_r$

$$N = 1.0e + 05, \phi = 0.80, \tilde{v} = 1.00e - 02, r_{min} = 1.00e + 00, r_{max} = 2.00e + 01$$

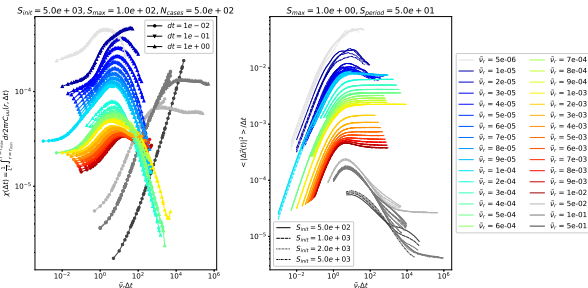


Figure: Comparison of displacement cooperativities $\chi(\Delta t)$ and mean square displacements divided by lag times $\langle |\Delta \vec{r}(\Delta t)|^2 \rangle / \Delta t$, at packing fraction $\phi = 0.80$ and self-propulsion velocity $\tilde{v} = 1 \cdot 10^{-2}$.

Subdiffusive behaviour and ageing effect characteristic of glassiness

- at high activity (phase-separated regime),
- at very low activity (glass phase).

Displacement cooperativity with varying $\tilde{\nu}$

$$N = 1.0e+05, \phi = 1.00, \tilde{\nu}_r = 3.00e-04, r_{min} = 1.00e+00, r_{max} = 2.00e+01$$

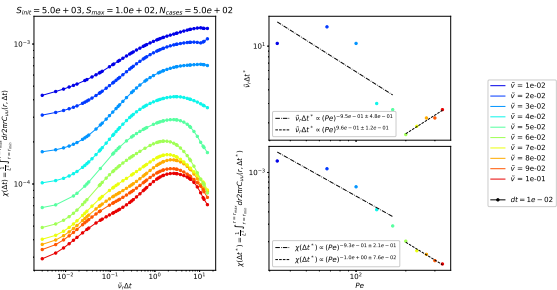


Figure: Comparison of displacement cooperativities $\chi(\Delta t)$, number of rotations of maximum cooperativity $\tilde{\nu}_r \Delta t^*$ and maximum cooperativities $\chi(\Delta t^*)$, at packing fraction $\phi = 1.00$ and self-propulsion velocity $\tilde{\nu}_r = 3 \cdot 10^{-4}$.

- Change of $\tilde{\nu}_r \Delta t^*(\text{Pe})$ and $\chi(\Delta t^*, \text{Pe})$ slopes at MIPS.
- $(\tilde{\nu} \searrow \Leftrightarrow \text{Pe} \nearrow) \Rightarrow \chi(\Delta t^*) \searrow$
- Non-monotonous variations of $\tilde{\nu}_r \Delta t^*$ with Pe.

Ageing effect with varying \tilde{v}

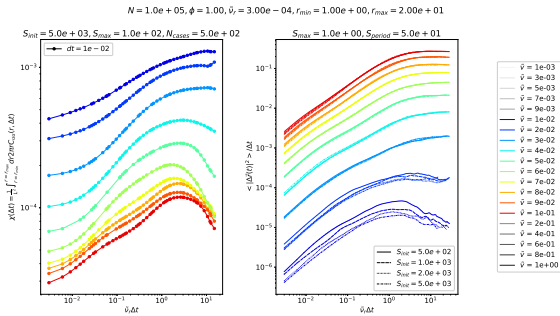


Figure: Comparison of displacement cooperativities $\chi(\Delta t)$ and mean square displacements divided by lag times $\langle |\Delta \vec{r}(\Delta t)|^2 \rangle / \Delta t$, at packing fraction $\phi = 1.00$ and rotation diffusion constant $\tilde{v}_r = 3 \cdot 10^{-4}$.

Subdiffusive behaviour and ageing effect characteristic of glassiness at low self-propulsion velocity (glass phase).

Directional displacement correlations

$$\vec{u}(\vec{r}, t, t + \Delta t) = \underbrace{\frac{\vec{u}(\vec{r}, t, t + \Delta t) \cdot \Delta \vec{r}}{||\Delta \vec{r}||} \frac{\Delta \vec{r}}{||\Delta \vec{r}||}}_{u_L(\vec{r}, t, t + \Delta t)} + \underbrace{\vec{u}(\vec{r}, t, t + \Delta t) - u_L(\vec{r}, t, t + \Delta t) \Delta \vec{r}}_{\vec{u}_T(\vec{r}, t, t + \Delta t)} \perp \Delta \vec{r}$$

Eric R Weeks, John C Crocker, and David A Weitz. "Short-and long-range correlated motion observed in colloidal glasses and liquids". In: *Journal of Physics: Condensed Matter* 19.20 (2007), p. 205131

Vishwas V Vasisht et al. "Rate Dependence of Elementary Rearrangements and Spatiotemporal Correlations in the 3D Flow of Soft Solids". In: *Physical review letters* 120.1 (2018), p. 018001

Directional displacement correlations

$$\vec{u}(\vec{r}, t, t + \Delta t) = \frac{\overbrace{\vec{u}(\vec{r}, t, t + \Delta t) \cdot \Delta \vec{r}}^{\text{u}_L(\vec{r}, t, t + \Delta t)} ||\Delta \vec{r}||}{||\Delta \vec{r}||} \frac{\Delta \vec{r}}{||\Delta \vec{r}||} + \underbrace{\vec{u}(\vec{r}, t, t + \Delta t) - u_L(\vec{r}, t, t + \Delta t) \Delta \vec{r}}_{\vec{u}_T(\vec{r}, t, t + \Delta t)} \perp \Delta \vec{r}$$

→ We can calculate displacement correlations in parallel and perpendicular directions to particles separations $\Delta \vec{r}$.

$$C_{uu}^L(\Delta \vec{r}, \Delta t) = \langle u_L(\vec{r} + \Delta \vec{r}, t, t + \Delta t) u_L(\vec{r}, t, t + \Delta t) \rangle$$

$$C_{uu}^T(\Delta \vec{r}, \Delta t) = \langle \vec{u}_T(\vec{r} + \Delta \vec{r}, t, t + \Delta t) \cdot \vec{u}_T(\vec{r}, t, t + \Delta t) \rangle$$

Eric R Weeks, John C Crocker, and David A Weitz. "Short-and long-range correlated motion observed in colloidal glasses and liquids". In: *Journal of Physics: Condensed Matter* 19.20 (2007), p. 205131

Vishwas V Vasisht et al. "Rate Dependence of Elementary Rearrangements and Spatiotemporal Correlations in the 3D Flow of Soft Solids". In: *Physical review letters* 120.1 (2018), p. 018001

Directional displacement correlations with varying $\tilde{\nu}_r$

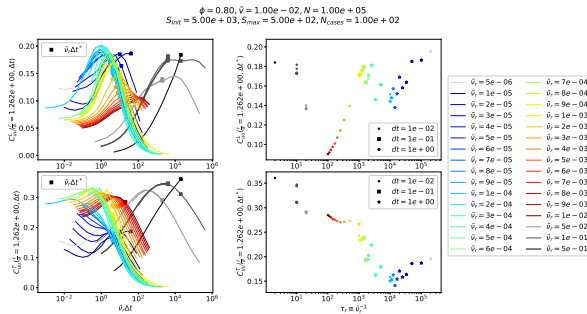


Figure: Comparison of longitudinal and transversal displacement correlations at grid size distance, $C_{uu}^L(\Delta t)$ and $C_{uu}^T(\Delta t)$, at packing fraction $\phi = 0.80$ and self-propulsion velocity $\tilde{\nu} = 1 \cdot 10^{-2}$.

Hard to interpret these raw data...

Directional displacement correlations with varying $\tilde{\nu}_r$

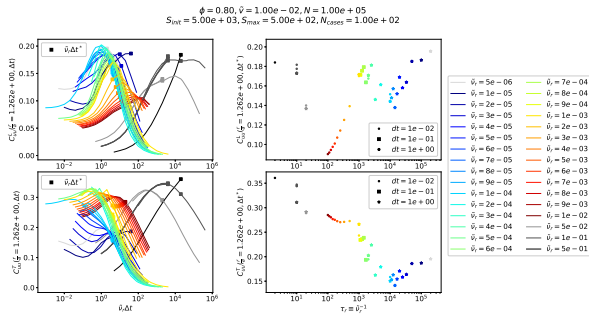


Figure: Comparison of longitudinal and transversal displacement correlations at grid size distance, $C_{uu}^L(\Delta t)$ and $C_{uu}^T(\Delta t)$, at packing fraction $\phi = 0.80$ and self-propulsion velocity $\tilde{\nu} = 1 \cdot 10^{-2}$.

Hard to interpret these raw data... \Rightarrow look at the ratio!

Directional displacement correlations with varying $\tilde{\nu}_r$

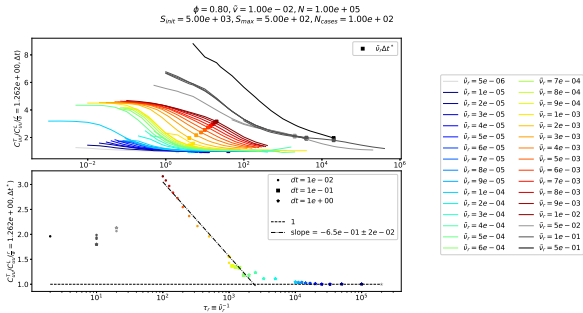


Figure: Comparison of ratio of transversal and longitudinal displacement correlations at grid size distance, $C_{uu}^T/C_{uu}^L(\Delta t)$, at packing fraction $\phi = 0.80$ and self-propulsion velocity $\tilde{v} = 1 \cdot 10^{-2}$.

- Clear change of $C_{uu}^T/C_{uu}^L(\Delta t^*, Pe)$ slope at MIPS.
- $C_{uu}^T/C_{uu}^L(\Delta t^* > 1$ in homogeneous fluid regime and $C_{uu}^T/C_{uu}^L(\Delta t^* = 1$ in phase separated state.

Directional displacement correlations with varying $\tilde{\nu}$

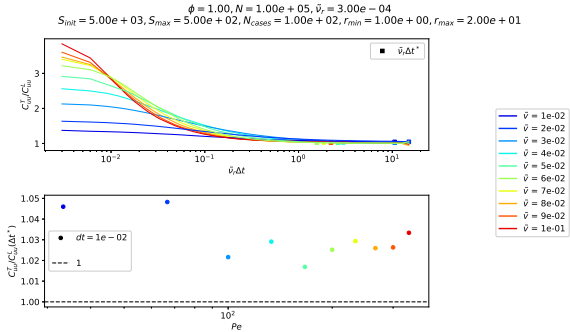


Figure: Comparison of ratio of transversal and longitudinal displacement correlations at grid size distance, $C_{uu}^T / C_{uu}^L(\Delta t)$, at packing fraction $\phi = 1.00$ and rotation diffusion constant $\tilde{\nu}_r = 3 \cdot 10^{-4}$.

- No clear change of $C_{uu}^T / C_{uu}^L(\Delta t^*, Pe)$ slope at MIPS.
- $C_{uu}^T / C_{uu}^L(\Delta t^*) \sim 1$ in both the homogeneous fluid regime and phase separated state.

Overview (varying $\tilde{\nu}_r$)

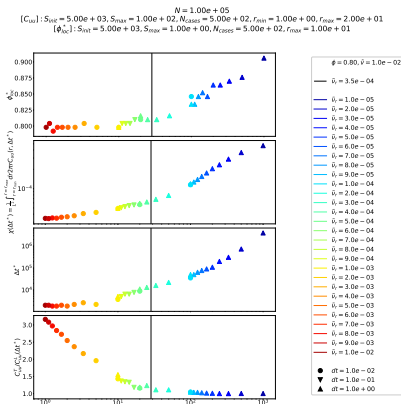


Figure: Overview plot of most probable local density ϕ_{loc}^* , maximum cooperativity $\chi(\Delta t^*)$, time of maximum cooperativity Δt^* and ratio of transversal and longitudinal displacement correlations at time of maximum cooperativity and grid size distance $C_{uu}^T/C_{uu}^L(\Delta t^*)$, at packing fraction $\phi = 0.80$ and self-propelling velocity $\tilde{\nu} = 1 \cdot 10^{-2}$.

Overview (varying $\tilde{\nu}_r$)

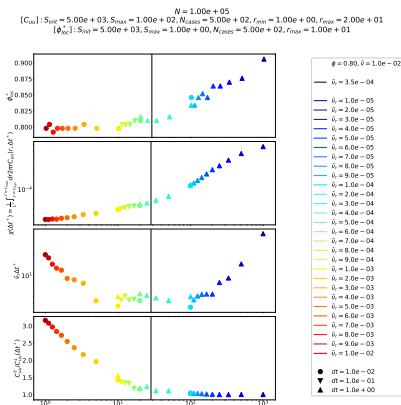


Figure: Overview plot of most probable local density ϕ_{loc}^* , maximum cooperativity $\chi(\Delta t^*)$, number of rotations of maximum cooperativity $\tilde{\nu}_r \Delta t^*$ and ratio of transversal and longitudinal displacement correlations at time of maximum cooperativity and grid size distance $C_{uu}^T/C_{uu}^L(\Delta t^*)$, at packing fraction $\phi = 0.80$ and self-propelling velocity $\tilde{v} = 1 \cdot 10^{-2}$.

Overview (varying \tilde{v})

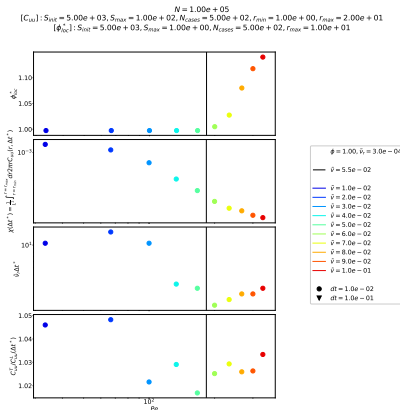


Figure: Overview plot of most probable local density ϕ_{loc}^* , maximum cooperativity $\chi(\Delta t^*)$, number of rotations of maximum cooperativity $\tilde{\nu}_r \Delta t^*$ and ratio of transversal and longitudinal displacement correlations at time of maximum cooperativity and grid size distance $C_{uu}^T/C_{uu}^L(\Delta t^*)$, at packing fraction $\phi = 1.00$ and rotation diffusion constant $\tilde{\nu}_r = 3 \cdot 10^{-4}$.

1 What is active matter?

2 Model and method

- Model
- Method

3 Observations

- Motility-induced phase separation
- Displacement correlations and cooperativities
- Shear strain correlations**

4 Conclusion

Trajectories at low activity

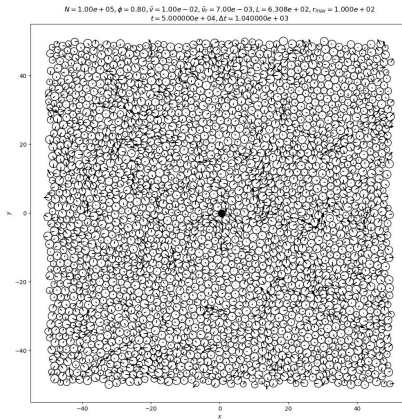


Figure: (Movie) Trajectories at low activity ($\tilde{\nu}_r = 7 \cdot 10^{-3}$) with $\Delta t = 1 \cdot 10^3$.

Trajectories at high activity

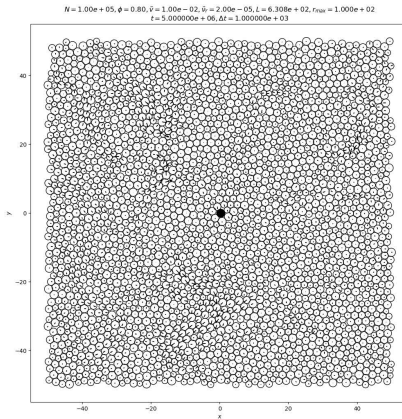


Figure: (Movie) Trajectories at high activity ($\tilde{\nu}_r = 2 \cdot 10^{-5}$) with $\Delta t = 1 \cdot 10^3$.

Linearised shear strain

$\vec{u}(\vec{r}, t, t + \Delta t) = \begin{pmatrix} u_x(\vec{r}, t, t + \Delta t) \\ u_y(\vec{r}, t, t + \Delta t) \end{pmatrix} \equiv$ displacement of particle at position \vec{r} between times t and $t + \Delta t$

Accumulated shear strain at position \vec{r} between times t and $t + \Delta t$

$$\varepsilon_{xy}(\vec{r}, t, t + \Delta t)$$

$$\frac{\|\vec{u}\|}{L} \ll 1 \quad \frac{1}{2} \left(\frac{\partial}{\partial x} u_y(\vec{r}, t, t + \Delta t) + \frac{\partial}{\partial y} u_x(\vec{r}, t, t + \Delta t) \right)$$

with L characteristic length of system.

Shear strain correlation

$$C_{\varepsilon_{xy}\varepsilon_{xy}}(\Delta\vec{r}, \Delta t) = \langle \varepsilon_{xy}(\vec{r} + \Delta\vec{r}, t, t + \Delta t) \varepsilon_{xy}(\vec{r}, t, t + \Delta t) \rangle$$

Shear strain correlation

$$\begin{aligned} C_{\varepsilon_{xy}\varepsilon_{xy}}(\Delta\vec{r}, \Delta t) &= \langle \varepsilon_{xy}(\vec{r} + \Delta\vec{r}, t, t + \Delta t) \varepsilon_{xy}(\vec{r}, t, t + \Delta t) \rangle \\ &= \frac{\int dt \int d^2\vec{r} \varepsilon_{xy}(\vec{r}, t, t + \Delta t) \varepsilon_{xy}(\vec{r} + \Delta\vec{r}, t, t + \Delta t)}{\int dt \int d^2\vec{r} |\varepsilon_{xy}(\vec{r}, t, t + \Delta t)|^2} \end{aligned}$$

Shear strain correlation

$$\begin{aligned} C_{\varepsilon_{xy}\varepsilon_{xy}}(\Delta\vec{r}, \Delta t) &= \langle \varepsilon_{xy}(\vec{r} + \Delta\vec{r}, t, t + \Delta t) \varepsilon_{xy}(\vec{r}, t, t + \Delta t) \rangle \\ &= \frac{\int dt \int d^2\vec{r} \varepsilon_{xy}(\vec{r}, t, t + \Delta t) \varepsilon_{xy}(\vec{r} + \Delta\vec{r}, t, t + \Delta t)}{\int dt \int d^2\vec{r} |\varepsilon_{xy}(\vec{r}, t, t + \Delta t)|^2} \\ &= \frac{\mathcal{F}^{-1} \left\{ \int dt |\mathcal{F}\{\varepsilon_{xy}\}(\vec{k}, t, t + \Delta t)|^2 \right\} (\Delta\vec{r}, \Delta t)}{\int dt \int d^2\vec{r} ||\varepsilon_{xy}(\vec{r}, t, t + \Delta t)||^2} \end{aligned}$$

Projection of shear strain correlation

Symmetrised gradient \Rightarrow four-fold symmetry of $C_{\varepsilon_{xy}\varepsilon_{xy}}(\Delta\vec{r}, \Delta t)$.

Projection of shear strain correlation

Symmetrised gradient \Rightarrow four-fold symmetry of $C_{\varepsilon_{xy}\varepsilon_{xy}}(\Delta\vec{r}, \Delta t)$.

$$C_4^4(\Delta r, \Delta t) = \frac{1}{\pi} \int_0^{2\pi} d\theta \cos(4\theta) C_{\varepsilon_{xy}\varepsilon_{xy}}(\Delta\vec{r} \equiv (\Delta r, \theta), \Delta t)$$

Projection of shear strain correlation

Symmetrised gradient \Rightarrow four-fold symmetry of $C_{\varepsilon_{xy}\varepsilon_{xy}}(\Delta\vec{r}, \Delta t)$.

$$C_4^4(\Delta r, \Delta t) = \frac{1}{\pi} \int_0^{2\pi} d\theta \cos(4\theta) C_{\varepsilon_{xy}\varepsilon_{xy}}(\Delta\vec{r} \equiv (\Delta r, \theta), \Delta t)$$
$$\underset{\frac{\Delta r}{a} \gg 1}{\propto} \frac{1}{\Delta r^2} \quad (\text{elastic medium})$$

with $a \equiv$ average interparticle distance.

Real space method

Shear strains are evaluated on a grid to calculate their correlations.

$$\vec{u}(\vec{r}_i, t, t + \Delta t) \xrightarrow{\text{coarse-graining}} \varepsilon_{xy,ij}(t, t + \Delta t)$$

(Gaussian)

Real space method

Shear strains are evaluated on a grid to calculate their correlations.

$$\vec{u}(\vec{r}_i, t, t + \Delta t) \xrightarrow[\text{coarse-graining}]{\text{(Gaussian)}} \varepsilon_{xy,ij}(t, t + \Delta t) \xrightarrow{\text{FFT}} C_{\varepsilon_{xy}\varepsilon_{xy},ij}$$

Shear strain map at high activity (real space method)

$N = 1.00e + 05$, $\phi = 0.80$, $\tilde{v} = 1.00e - 02$, $\tilde{\nu}_r = 2.00e - 05$, $\tilde{N} = 1.00e + 05$, $\Delta t = 1.00e + 03$, $nD_0\Delta t = 6.28e + 02$
 $L = 6.31e + 02$, $x_0 = 0.00e + 00$, $y_0 = 0.00e + 00$, $S_{int} = 5.00e + 03$, $S_{max} = 1.00e + 00$, $N_{cases} = 5.00e + 02$, $r_{cut} = 2.00e + 00$, $\sigma = 2.00e + 00$

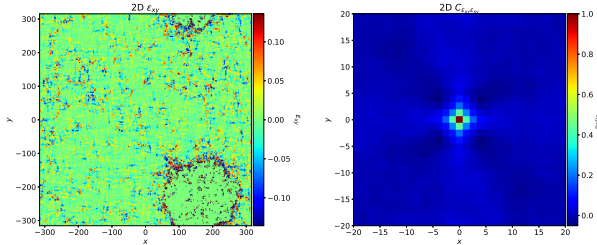


Figure: Shear strain map $\epsilon_{xy}(\vec{r}, t, t + \Delta t)$ and corresponding shear strain correlations $C_{\epsilon_{xy}\epsilon_{xy}}(\Delta \vec{r}, \Delta t)$, at packing fraction $\phi = 0.80$, self-propulsion velocity $\tilde{v} = 1 \cdot 10^{-2}$ and rotation diffusion constant $\tilde{\nu}_r = 2 \cdot 10^{-5}$.

- Highest strain values at phase interface.
- Quadropolar symmetry of shear strain correlations.
- Shear strain correlations blurred because of gas phase.

Real space method

Shear strains are evaluated on a grid to calculate their correlations.

$$\vec{u}(\vec{r}_i, t, t + \Delta t) \xrightarrow[\text{coarse-graining}]{\quad} \varepsilon_{xy,ij}(t, t + \Delta t) \xrightarrow[\text{FFT}]{\quad} C_{\varepsilon_{xy}\varepsilon_{xy},ij}$$

(Gaussian)

Significant downside: coarse-graining step is particularly long,
execution time = days to get good statistics.

Real space method

Shear strains are evaluated on a grid to calculate their correlations.

$$\vec{u}(\vec{r}_i, t, t + \Delta t) \xrightarrow[\text{coarse-graining}]{\text{(Gaussian)}} \varepsilon_{xy,ij}(t, t + \Delta t) \xrightarrow{\text{FFT}} C_{\varepsilon_{xy}\varepsilon_{xy},ij}$$

Significant downside: coarse-graining step is particularly long,
execution time = days to get good statistics.
⇒ turn to a Fourier space based method to speed up this part.

Collective mean square displacements

$$\vec{u}(\vec{r}, t, t + \Delta t) \xrightarrow{\text{Fourier transform}} \tilde{\vec{u}}(\vec{k}, t, t + \Delta t)$$

Bernd Illing et al. "Strain pattern in supercooled liquids". In: *Physical review letters* 117.20 (2016), p. 208002

F Leonforte et al. "Continuum limit of amorphous elastic bodies. iii. three-dimensional systems". In: *Physical Review B* 72.22 (2005), p. 224206

Collective mean square displacements

$$\vec{u}(\vec{r}, t, t + \Delta t) \xrightarrow{\text{Fourier transform}} \tilde{\vec{u}}(\vec{k}, t, t + \Delta t)$$

$$C^\perp(\vec{k}, \Delta t) = ||\vec{k}||^{-2} \left\langle ||\vec{k} \wedge \tilde{\vec{u}}(\vec{k}, t, t + \Delta t)||^2 \right\rangle$$

$$C^\parallel(\vec{k}, \Delta t) = ||\vec{k}||^{-2} \left\langle ||\vec{k} \cdot \tilde{\vec{u}}(\vec{k}, t, t + \Delta t)||^2 \right\rangle$$

respectively the transversal and longitudinal collective mean square displacements (CMSD).

Bernd Illing et al. "Strain pattern in supercooled liquids". In: *Physical review letters* 117.20 (2016), p. 208002

F Leonforte et al. "Continuum limit of amorphous elastic bodies. iii. three-dimensional systems". In: *Physical Review B* 72.22 (2005), p. 224206

Collective mean square displacements

$$\vec{u}(\vec{r}, t, t + \Delta t) \xrightarrow{\text{Fourier transform}} \tilde{\vec{u}}(\vec{k}, t, t + \Delta t)$$

$$C^\perp(\vec{k}, \Delta t) = ||\vec{k}||^{-2} \left\langle ||\vec{k} \wedge \tilde{\vec{u}}(\vec{k}, t, t + \Delta t)||^2 \right\rangle \xrightarrow{\text{isotropy}} C^\perp(k, \Delta t)$$

$$C^\parallel(\vec{k}, \Delta t) = ||\vec{k}||^{-2} \left\langle ||\vec{k} \cdot \tilde{\vec{u}}(\vec{k}, t, t + \Delta t)||^2 \right\rangle \xrightarrow{\text{isotropy}} C^\parallel(k, \Delta t)$$

respectively the transversal and longitudinal collective mean square displacements (CMSD).

Bernd Illing et al. "Strain pattern in supercooled liquids". In: *Physical review letters* 117.20 (2016), p. 208002

F Leonforte et al. "Continuum limit of amorphous elastic bodies. iii. three-dimensional systems". In: *Physical Review B* 72.22 (2005), p. 224206

CMSD and shear strain correlations

$$C_{\varepsilon_{xy}\varepsilon_{xy}}(\Delta\vec{r}, \Delta t) = \mathcal{F}^{-1} \left\{ -\frac{k_x^2 k_y^2}{k^2} \left(C^\perp(k, \Delta t) - C^{\parallel}(k, \Delta t) \right) + \frac{k^2}{4} C^\perp(k, \Delta t) \right\}(\Delta\vec{r}, \Delta t)$$

Bernd Illing et al. "Strain pattern in supercooled liquids". In: *Physical review letters* 117.20 (2016), p. 208002

F Leonforte et al. "Continuum limit of amorphous elastic bodies. iii. three-dimensional systems". In: *Physical Review B* 72.22 (2005), p. 224206

CMSD and shear strain correlations

$$C_{\varepsilon_{xy}\varepsilon_{xy}}(\Delta\vec{r}, \Delta t) = \mathcal{F}^{-1} \left\{ -\frac{k_x^2 k_y^2}{k^2} \left(C^\perp(k, \Delta t) - C^{\parallel}(k, \Delta t) \right) + \frac{k^2}{4} C^\perp(k, \Delta t) \right\} (\Delta\vec{r}, \Delta t)$$

$$\begin{aligned} C^{\parallel}(k, \Delta t) &= 0 \\ C^\perp(k, \Delta t) &\propto k^{-2} \end{aligned} \quad (\text{incompressible glass})$$

Bernd Illing et al. "Strain pattern in supercooled liquids". In: *Physical review letters* 117.20 (2016), p. 208002

F Leonforte et al. "Continuum limit of amorphous elastic bodies. iii. three-dimensional systems". In: *Physical Review B* 72.22 (2005), p. 224206

CMSD and shear strain correlations

$$C_{\varepsilon_{xy}\varepsilon_{xy}}(\Delta \vec{r}, \Delta t) = \mathcal{F}^{-1} \left\{ -\frac{k_x^2 k_y^2}{k^2} \left(C^\perp(k, \Delta t) - C^{\parallel}(k, \Delta t) \right) + \frac{k^2}{4} C^\perp(k, \Delta t) \right\} (\Delta \vec{r}, \Delta t)$$

$$\begin{aligned} C^{\parallel}(k, \Delta t) &= 0 && \text{(incompressible glass)} \\ C^\perp(k, \Delta t) &\propto k^{-2} \\ \Rightarrow C_{\varepsilon_{xy}\varepsilon_{xy}}(\Delta \vec{r}, \Delta t) &\propto \cos(4\theta) \Delta r^{-2} \end{aligned}$$

Bernd Illing et al. "Strain pattern in supercooled liquids". In: *Physical review letters* 117.20 (2016), p. 208002

F Leonforte et al. "Continuum limit of amorphous elastic bodies. iii. three-dimensional systems". In: *Physical Review B* 72.22 (2005), p. 224206

CMSD method

Displacements are put on a grid to calculate shear strain correlations from CMSD.

$$\vec{u}(\vec{r}_i, t, t + \Delta t) \xrightarrow{\text{coarse-graining}} \vec{u}_{ij}(t, t + \Delta t)$$

(average in grid box)

CMSD method

Displacements are put on a grid to calculate shear strain correlations from CMSD.

$$\vec{u}(\vec{r}_i, t, t + \Delta t) \xrightarrow[\text{coarse-graining}]{\quad} \vec{u}_{ij}(t, t + \Delta t) \xrightarrow{\text{FFT}} \tilde{\vec{u}}_{ij}(t, t + \Delta t)$$

(average in grid box)

CMSD method

Displacements are put on a grid to calculate shear strain correlations from CMSD.

$$\vec{u}(\vec{r}_i, t, t + \Delta t) \rightarrow \vec{u}_{ij}(t, t + \Delta t) \xrightarrow{\text{FFT}} \tilde{\vec{u}}_{ij}(t, t + \Delta t) \rightarrow \text{CMSD}$$

CMSD at high activity

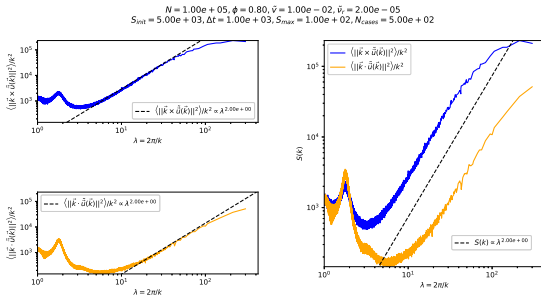


Figure: Transversal and longitudinal CMSD, $C^\perp(k, \Delta t) \equiv \langle ||\vec{k} \wedge \tilde{u}(\vec{k})||^2 \rangle / k^2$ and $C^\parallel(k, \Delta t) \equiv \langle ||\vec{k} \cdot \tilde{u}(\vec{k})||^2 \rangle / k^2$, at packing fraction $\phi = 0.80$, self-propulsion velocity $\tilde{v} = 1 \cdot 10^{-2}$ and rotation diffusion constant $\tilde{\nu}_r = 2 \cdot 10^{-5}$.

- $C^\parallel(k, \Delta t) \neq 0$.
- $C^\perp(k, \Delta t), C^\parallel(k, \Delta t) \propto k^{-2}$ for \sim a decade, limited for small k by finite-size effect and for large k by microscopic structure.

CMSD at low activity

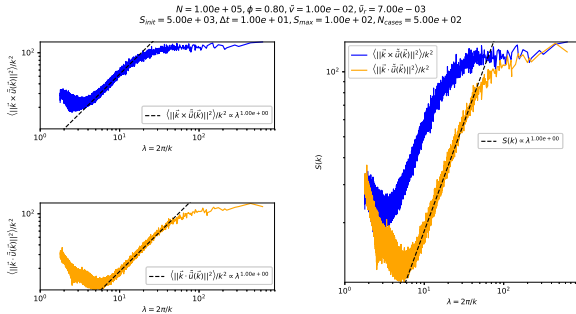


Figure: Transversal and longitudinal CMSD, $C^\perp(k, \Delta t) \equiv \left\langle \left| \vec{k} \times \tilde{\vec{u}}(\vec{k}) \right|^2 \right\rangle / k^2$ and $C^{\parallel}(k, \Delta t) \equiv \left\langle \left| \vec{k} \cdot \tilde{\vec{u}}(\vec{k}) \right|^2 \right\rangle / k^2$, at packing fraction $\phi = 0.80$, self-propulsion velocity $\tilde{v} = 1 \cdot 10^{-2}$ and rotation diffusion constant $\tilde{v}_r = 7 \cdot 10^{-3}$.

→ $C^\perp(k, \Delta t), C^{\parallel}(k, \Delta t) \propto k^{-1}$ for \sim a decade, limited for small k by finite-size effect and for large k by microscopic structure.

CMSD method

Displacements are put on a grid to calculate shear strain correlations from CMSD.

$$\vec{u}(\vec{r}_i, t, t + \Delta t) \rightarrow \vec{u}_{ij}(t, t + \Delta t) \xrightarrow{\text{FFT}} \tilde{\vec{u}}_{ij}(t, t + \Delta t) \rightarrow \text{CMSD}$$

$$\text{CMSD} \xrightarrow[\text{Gaussian filter}]{} \text{filtered CMSD} \xrightarrow[\text{FFT}^{-1}]{} C_{\varepsilon_{xy}\varepsilon_{xy}}(\Delta \vec{r}, \Delta t)$$

A Gaussian filter is used to filter out effects of the microscopic structure of the system.

CMSD method

Displacements are put on a grid to calculate shear strain correlations from CMSD.

$$\vec{u}(\vec{r}_i, t, t + \Delta t) \rightarrow \vec{u}_{ij}(t, t + \Delta t) \xrightarrow{\text{FFT}} \tilde{\vec{u}}_{ij}(t, t + \Delta t) \rightarrow \text{CMSD}$$

$$\text{CMSD} \rightarrow \text{filtered CMSD} \rightarrow C_{\varepsilon_{xy}\varepsilon_{xy}}(\Delta \vec{r}, \Delta t) \xrightarrow{\substack{\text{projection} \\ \text{on } \cos(4\theta)}} C_4^4(\Delta r, \Delta t)$$

A Gaussian filter is used to filter out effects of the microscopic structure of the system.

Projected strain correlations from CMSD at high activity

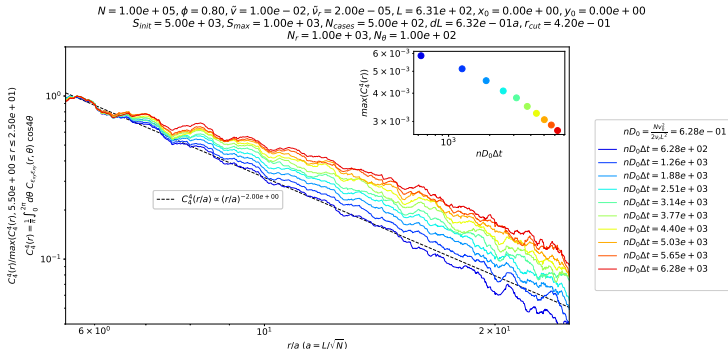


Figure: Rescaled projections of shear strain correlations $C_4^4(\Delta r, \Delta t)$, at packing fraction $\phi = 0.80$, self-propulsion velocity $\tilde{v} = 1 \cdot 10^{-2}$ and rotation diffusion constant $\tilde{\nu}_r = 2 \cdot 10^{-5}$.

→ Algebraic decay at low lag time with exponential cut-off.

Projected strain correlations from CMSD at high activity

$N = 1.00e + 05$, $\phi = 0.80$, $\tilde{v} = 1.00e - 02$, $\tilde{v}_r = 2.00e - 05$, $L = 6.31e + 02$, $x_0 = 0.00e + 00$, $y_0 = 0.00e + 00$
 $S_{init} = 5.00e + 03$, $S_{max} = 1.00e + 03$, $N_{cases} = 5.00e + 02$, $dL = 6.32e - 01a$, $r_{cut} = 4.20e - 01$
 $N_r = 1.00e + 03$, $N_\theta = 1.00e + 02$

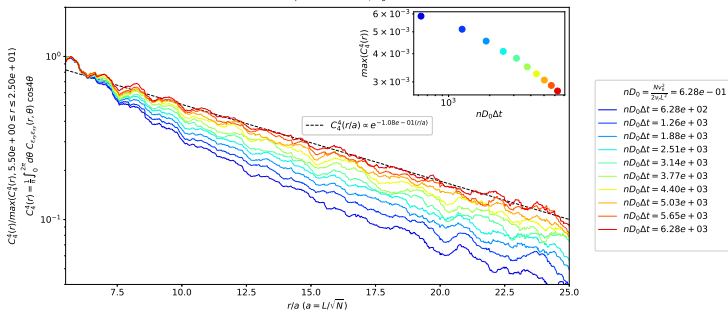


Figure: Rescaled projections of shear strain correlations $C_4^4(\Delta r, \Delta t)$, at packing fraction $\phi = 0.80$, self-propulsion velocity $\tilde{v} = 1 \cdot 10^{-2}$ and rotation diffusion constant $\tilde{v}_r = 2 \cdot 10^{-5}$.

→ Exponential decay at high lag time.

Projected strain correlations from CMSD at low activity

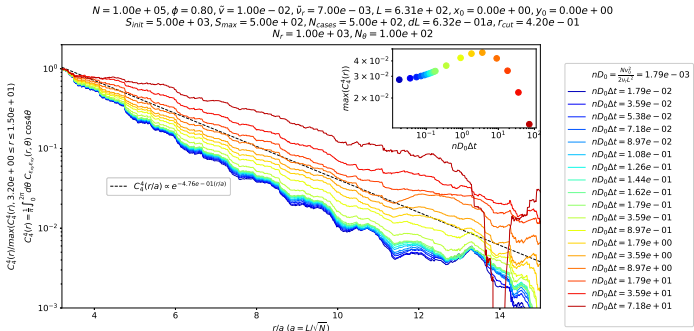


Figure: Rescaled projections of shear strain correlations $C_4^4(\Delta r, \Delta t)$, at packing fraction $\phi = 0.80$, self-propulsion velocity $\tilde{v} = 1 \cdot 10^{-2}$ and rotation diffusion constant $\tilde{\nu}_r = 7 \cdot 10^{-3}$.

- Exponential decay at all lag times.
- Exponential decay length scale around $2a$ and increasing function of lag time.

1 What is active matter?

2 Model and method

- Model
- Method

3 Observations

- Motility-induced phase separation
- Displacement correlations and cooperativities
- Shear strain correlations

4 Conclusion

Conclusion

- Active matter system displaying motility-induced phase separation.

Conclusion

- Active matter system displaying motility-induced phase separation.
- At fixed self-propelling velocity, this transition is accompanied by increased cooperativity \Rightarrow increased dynamical heterogeneity.
- While at fixed rotation diffusion constant, it is accompanied by decreased cooperativity.

Conclusion

- Active matter system displaying motility-induced phase separation.
- At fixed self-propelling velocity, this transition is accompanied by increased cooperativity \Rightarrow increased dynamical heterogeneity.
- While at fixed rotation diffusion constant, it is accompanied by decreased cooperativity.
 - \Rightarrow Péclet number is not enough to characterise the variations of the cooperativity and time of maximum cooperativity.

Conclusion

- Active matter system displaying motility-induced phase separation.
- At fixed self-propelling velocity, this transition is accompanied by increased cooperativity \Rightarrow increased dynamical heterogeneity.
- While at fixed rotation diffusion constant, it is accompanied by decreased cooperativity.
 - \Rightarrow Péclet number is not enough to characterise the variations of the cooperativity and time of maximum cooperativity.
- Shear strain correlations show algebraic decay for phase-separated systems and exponential decay for homogenous fluid systems.

Outlook

- Explore other paths through phase space to understand variations of cooperativities.

Outlook

- Explore other paths through phase space to understand variations of cooperativities.
- Characterise the transition from exponential to algebraic decay in shear strain correlations.